Supplement of Atmos. Chem. Phys., 22, 8701–8723, 2022
https://doi.org/10.5194/acp-22-8701-2022-supplement

Atmospheric Chemistry and Physics
Open Access

Supplement of

Nine-year trends of PM_{10} sources and oxidative potential in a rural background site in France

Lucille Joanna Borlaza et al.

Correspondence to: Lucille Joanna Borlaza (lucille-joanna.borlaza@univ-grenoble-alpes.fr) and Jean-Luc Jaffrezo (jaffrezo@univ-grenoble-alpes.fr)

Table of Contents

S1. Calculation of major chemical components of PM_{10}

Organic matter (OM) is calculated by multiplying OC mass concentrations by a factor 1.8 based on findings obtained from previous studies (Favez et al., 2010; Putaud et al., 2010). Sea salt sulfate (ss-sulfate) is calculated by multiplying the mass concentration of sodium by a factor of 0.252. The non-sea salt sulfate (nss-sulfate) corresponds to the sea salt sulfate subtracted from the total mass of sulfate using the factor from Seinfeld and Pandis (1998). Sea salt is estimated based on the mass concentrations of sodium chloride (Putaud et al., 2010). Dust is calculated based on calcium of non-sea-salt origin, following the empirical expression in (Putaud et al., 2004). Non-dust elements correspond to the sum of the other common measured trace elements other than geological ones (Salameh et al., 2015)).

$$[PM_{10}] = [OM] + [EC] + [nss-sulfate] + [nitrates] + [ammonium] + [sea\ salt] + [dust] + [non-dust]$$

(Eq. S1)

where:

$$[nss-sulfate] = [SO_4^{2-}] - 0.252[Na^+]$$
$$[sea\ salt] = [Cl^-] + 1.47[Na^+]$$
$$[dust] = 5.6 * [nss-Ca^{2+}]$$
$$[nss-Ca^{2+}] = [Ca^{2+}] - [Na^+]/26$$
$$[non-dust] = [Cu] + [Ni] + [Pb] + [V] + [Zn]$$

Table S1. Summary of quantification limits (QL) of each chemical specie measured in the OPE site.

Specie	Unit	Quantification limit (QL)
OC	µg m^{-3}	0.096
EC	µg m^{-3}	0.002
TC	µg m^{-3}	0.094
Cellulose	ng m^{-3}	6.500
MSA	ng m^{-3}	0.227
Cl^-	ng m^{-3}	4.451
NO_3^-	ng m^{-3}	24.820
SO_4^{2-}	ng m^{-3}	5.027
Na^+	ng m^{-3}	4.805
NH_4^+	ng m^{-3}	13.342
K^+	ng m^{-3}	1.628
Mg^{2+}	ng m^{-3}	0.344
Ca^{2+}	ng m^{-3}	5.014
Arabitol	ng m^{-3}	0.554
Sorbitol	ng m^{-3}	0.337
Mannitol	ng m^{-3}	0.356
Levoglucosan	ng m^{-3}	1.351
Mannosan	ng m^{-3}	0.352
Al	ng m^{-3}	25.440
As	ng m^{-3}	0.013
Ba	ng m^{-3}	1.708
Ca	ng m^{-3}	110.347
Cd	ng m^{-3}	0.023
Ce	ng m^{-3}	0.045
Co	ng m^{-3}	0.020

Cr	ng m^{-3}	1.077
Cs	ng m^{-3}	0.015
Cu	ng m^{-3}	0.220
Fe	ng m^{-3}	11.243
K	ng m^{-3}	10.705
La	ng m^{-3}	0.029
Li	ng m^{-3}	0.142
Mg	ng m^{-3}	13.000
Mn	ng m^{-3}	0.322
Mo	ng m^{-3}	3.146
Na	ng m^{-3}	27.735
Ni	ng m^{-3}	0.643
Pb	ng m^{-3}	0.048
Pd	ng m^{-3}	0.040
Pt	ng m^{-3}	0.013
Rb	ng m^{-3}	0.026
Sb	ng m^{-3}	0.051
Sc	ng m^{-3}	0.078
Se	ng m^{-3}	0.050
Sn	ng m^{-3}	0.403
Sr	ng m^{-3}	0.117
Ti	ng m^{-3}	0.453
Tl	ng m^{-3}	0.013
V	ng m^{-3}	0.018
Zn	ng m^{-3}	1.157
Zr	ng m^{-3}	0.627

S2. PMF model description

The PMF model is based on a factorial analysis that takes into account the evolution of the concentration of the measured chemical species and gathers, in the same factor, the fractions of the species evolving in the same way. Each factor will then be assigned to a source by the user based on literature data and geochemical knowledge of source characteristics in terms of trace chemical species.

The application of this model does not require prior knowledge of the chemical profiles of the sources, but its application must be performed on a large dataset (many chemical species, including in particular tracers and indicators of major sources) and on a large time series of samples. This is particularly the case for this study, to our knowledge among the largest datasets in the Europe. The general equation used in this PMF model is the following:

$$x_{ij} = (\sum_{k=1}^{p} g_{ik} \times f_{kj}) + e_{ij} \quad \text{(Eq. S2)}$$

Where x_{ij} : species concentration j for sample i

g_{ik} : factor contribution k for sample i

f_{kj} : factor contribution k from the specie j

e_{ij} : specie contribution j for sample i not explained by the model

This can be expressed in a matrix form simply by Eq. S3:

$$X = G \cdot F + E \quad \text{(Eq. S3)}$$

The model seeks to minimize the matrix E weighted by the matrix S containing the measurement uncertainties, i.e. Q=E/S. The S-matrix is calculated using Eq. S4 proposed by (Gianini et al., 2012):

$$s_{ij} = \sqrt{(DL_j)^2 + (CV_j \times x_{ij})^2 + (CV_{PM} \times x_{ij})^2} \quad \text{(Eq. S4)}$$

Where : DL_j : the limit of detection for species j (2 times the standard deviation of blanks)

CV_j : the coefficient of variation of specie j (calculated from several successive analyses of the same sample)

CV_{PM} : the additional coefficient of variation representing additional uncertainties by chemical species category

For some species, it was necessary to use an expanded uncertainty that takes into account analytical error and sampling error, which can be used instead of the methodology proposed by (Gianini et al., 2012). An uncertainty of $\frac{5}{6} \times DL$ was used for values <DL and the uncertainties that are four times the specie concentration geometric mean were attributed to missing or replaced values.

The robustness of the final PMF solution was evaluated using various statistical parameters based on the European guide on air pollution source apportionment with receptor models (Belis et al., 2014) and the geochemical soundness of the solution. In brief, the parameters are listed as follows:

- ✓ Evolution of the ratio Qtrue/Qrobust (<1.5)
- ✓ The weighted residuals are normally distributed for most of the species and between ±3 which should indicate good model results of most variables
- ✓ Evaluation of the statistical robustness of the optimal solution (sensitivity to noise and any random data point) using a bootstrap test (BS) for 100 successive iterations of the model and for a minimum correlation (r^2) of 0.6
- ✓ Evaluation of the geochemical soundness of the PMF-resolved factor profiles based on *a priori* knowledge of the chemical footprints of the sources, their specific tracers, the temporal variability (daily, weekly and seasonally), and the characteristics of the site studied
- ✓ Statistical evaluation and precision for constrained solutions using BS for 100 successive iterations of the model and for a minimum correlation (r^2) of 0.6
- ✓ There is no added extra uncertainty to the whole dataset

The Pearson distance and the Similarity Identity Distance (PD-SID):

To evaluate the stability of the chemical profile obtained in the OPE site against other sites in France, the Pearson distance (PD) and the Similarity Identity Distance (SID), following Belis et al. (2015), was used to perform a similarity assessment. The PD and SID defined by Eq. S5 and Eq. S6:

$PD = 1 - r^2$, where r is the Pearson coefficient (Eq. S5)

$\frac{\sqrt{2}}{n} \sum_{i=1}^{n} \frac{|a_i - b_i|}{a_i + b_i}$ (Eq. S6)

where a and b are the relative mass to PM_{10} of two different factors and n is the number of common species in a and b.

S3. Summary of PMF-resolved sources

Table S2. The PMF-resolved sources and their specific tracers

Identified factors	Specific tracers
Biomass burning	Levoglucosan, mannosan
Nitrate-rich	NO_3^-, NH_4^+
Sulfate-rich	SO_4^{2-}, NH_4^+
Mineral dust	Ca^{2+}, Al, Ti, Fe, Cu, Zn
Fresh sea salt	Na^+, Cl^-, Mg^{2+}
Aged sea salt	Na^+, Mg^{2+}
Primary biogenic	Polyols
MSA-rich	MSA
Traffic	EC, Cu, Sb, Sn

Table S3: Summary of the tested chemical constraints on source-specific tracers in the PMF factor profiles.

Factor profile	Element	Type	Value	Used in the final model
Biomass burning	Levoglucosan	Pull up maximally	(% dQ 0.50)	Yes
Biomass burning	Mannosan	Pull up maximally	(% dQ 0.50)	Yes
Primary biogenic	Levoglucosan	Set to zero	0	No
Primary biogenic	Mannosan	Set to zero	0	No
Primary biogenic	Polyols	Pull up maximally	(% dQ 0.50)	No
Primary biogenic	EC	Pull down maximally	(% dQ 0.50)	No
MSA-rich	MSA	Pull up maximally	(% dQ 0.50)	Yes
MSA-rich	Levoglucosan	Set to zero	0	Yes
MSA-rich	Mannosan	Set to zero	0	Yes
MSA-rich	Polyols	Pull down maximally	(% dQ 0.50)	No
MSA-rich	EC	Pull down maximally	(% dQ 0.50)	No
Nitrate-rich	Levoglucosan	Set to zero	0	No
Nitrate-rich	Mannosan	Set to zero	0	No
Mineral dust	Ti	Pull up maximally	(% dQ 0.50)	Yes
Primary traffic	Levoglucosan	Set to 0	0	Yes
Primary traffic	Mannosan	Set to 0	0	Yes
Primary traffic	Cu/Fe	Set to value	0.046 (% dQ 0.50)	No
Primary traffic	Cu/Sn	Set to value	5.6 (% dQ 0.50)	No
Primary traffic	Cu/Sb	Set to value	12.6 (% dQ 0.50)	No
Primary traffic	Cu/Mn	Set to value	5.7 (% dQ 0.50)	No
Primary traffic	OC*/EC	Set to value	0.44 (% dQ 0.50)	No

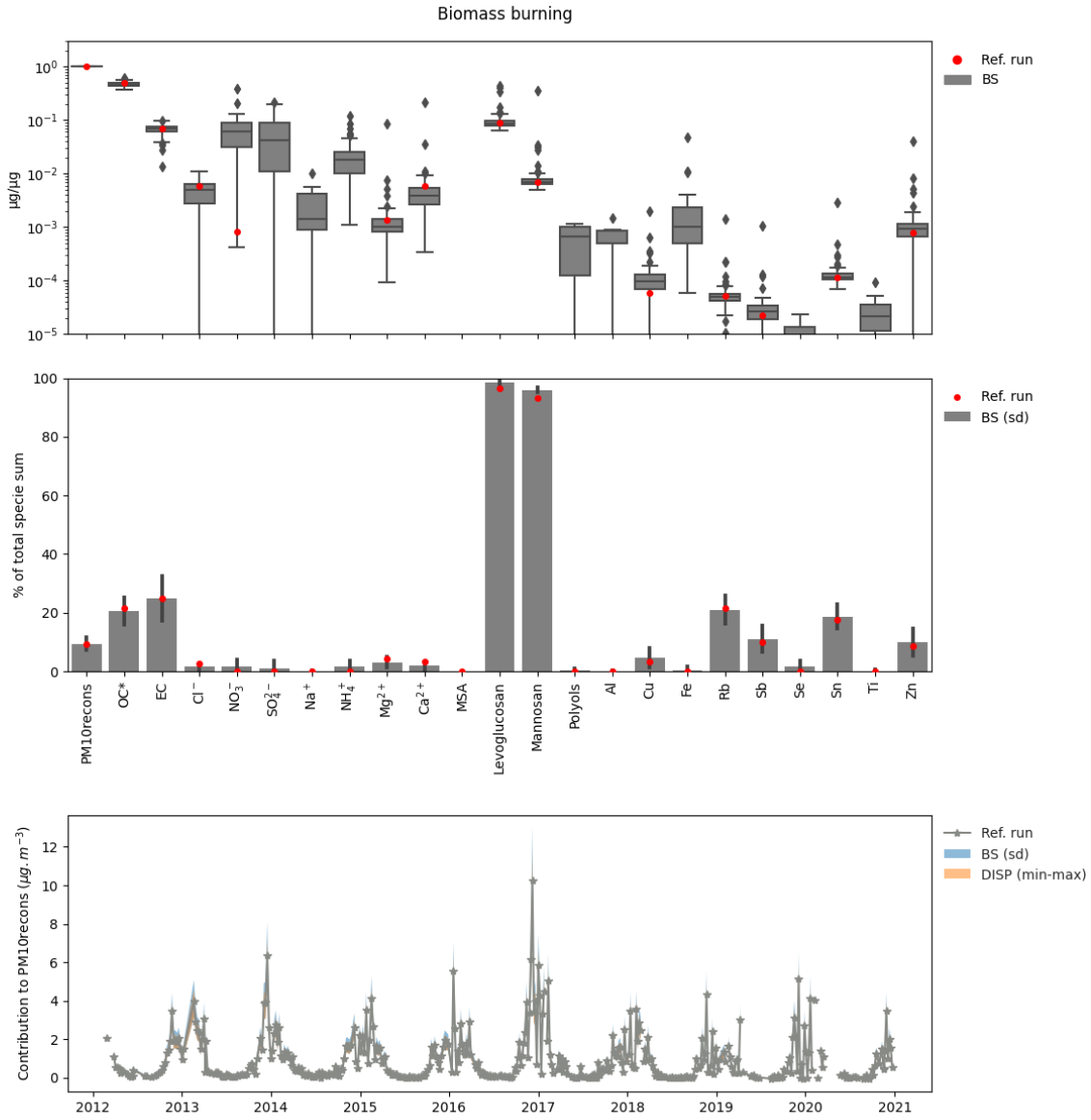

Figure S1: Chemical profile and temporal evolution with error estimates of the biomass burning factor

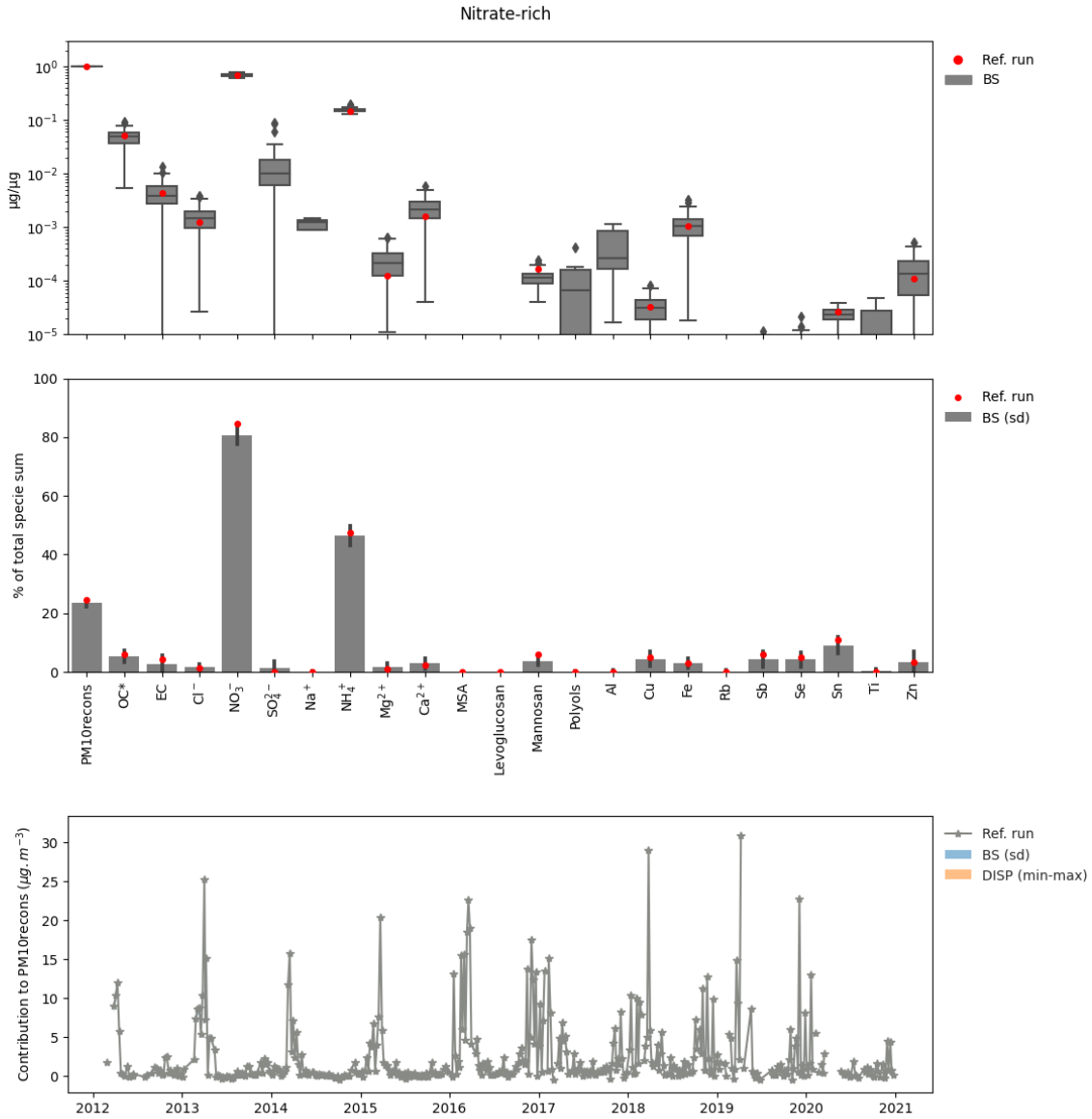

Figure S2: Chemical profile and temporal evolution with error estimates of the nitrate-rich factor

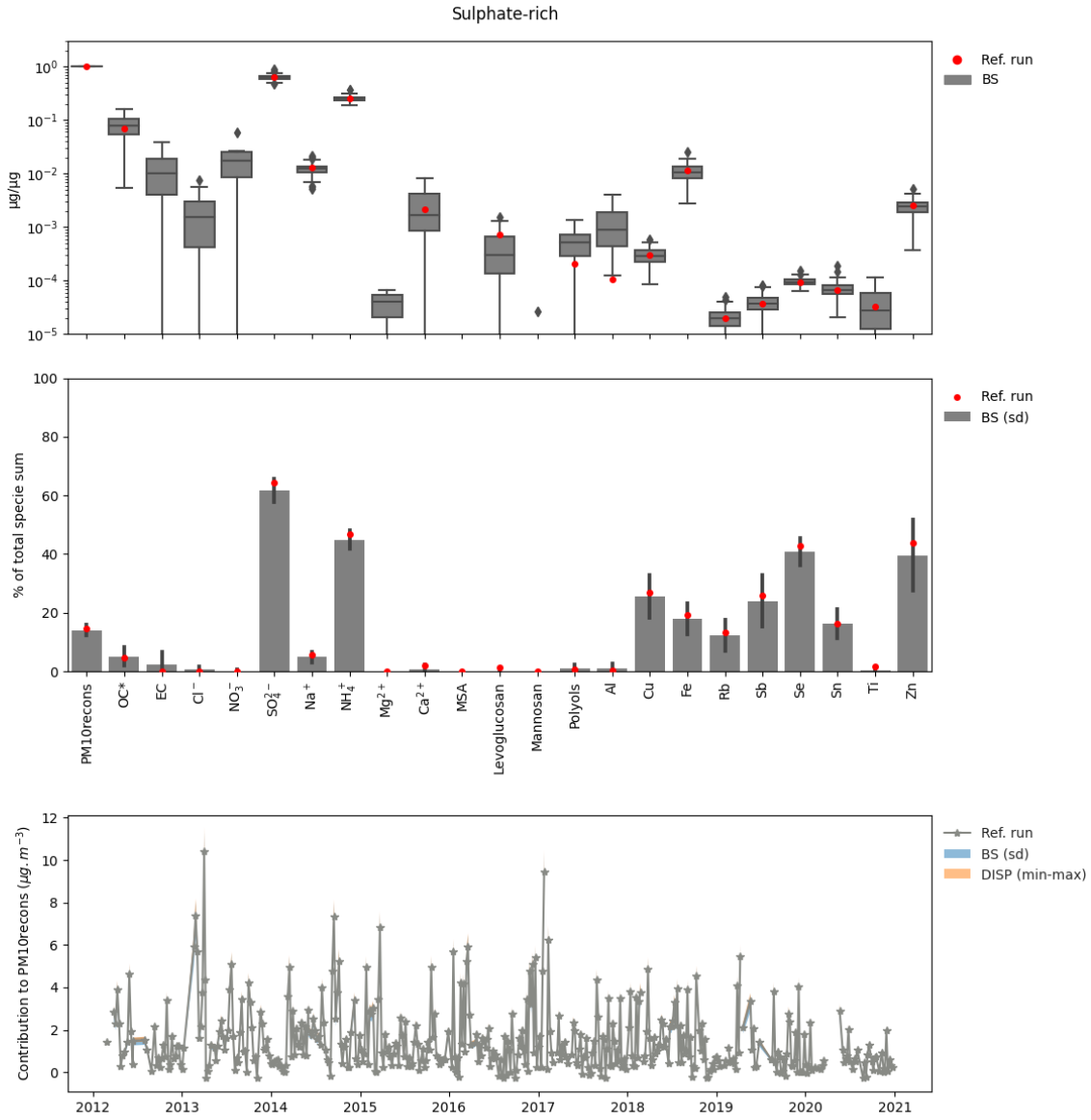

Figure S3: Chemical profile and temporal evolution with error estimates of the sulphate-rich factor

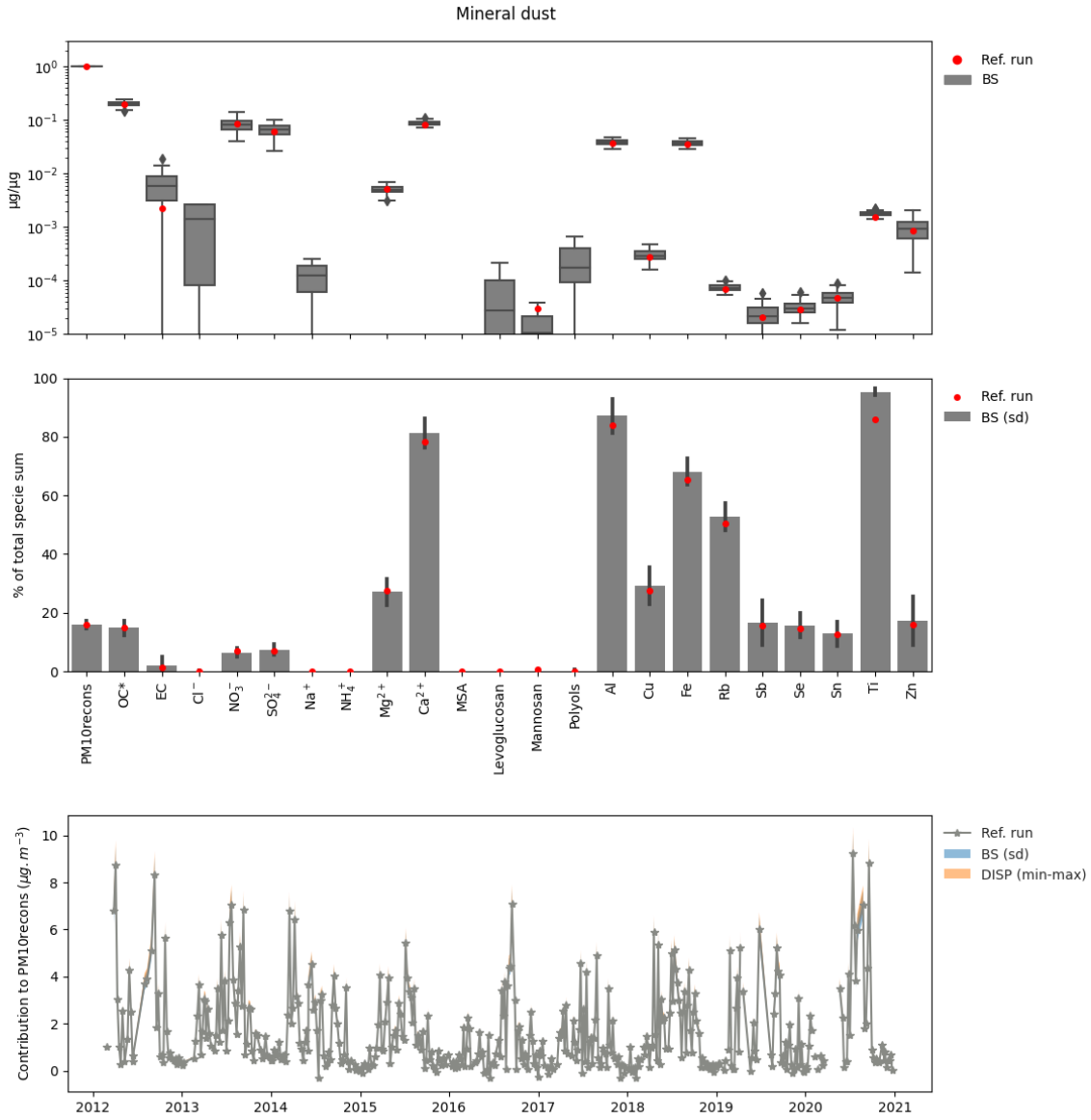

Figure S4: Chemical profile and temporal evolution with error estimates of the mineral dust factor

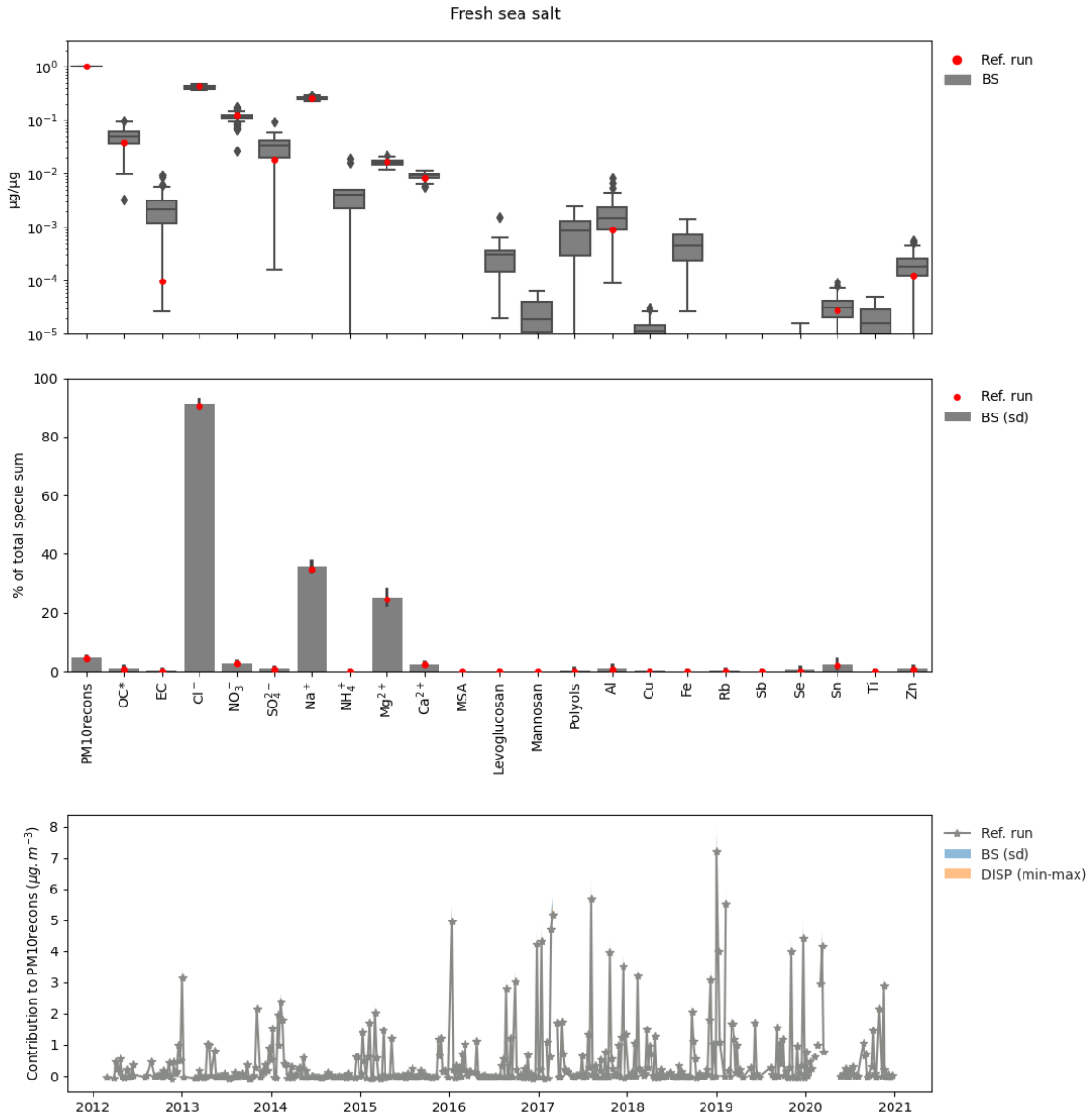

Figure S5: Chemical profile and temporal evolution with error estimates of the fresh sea salt factor

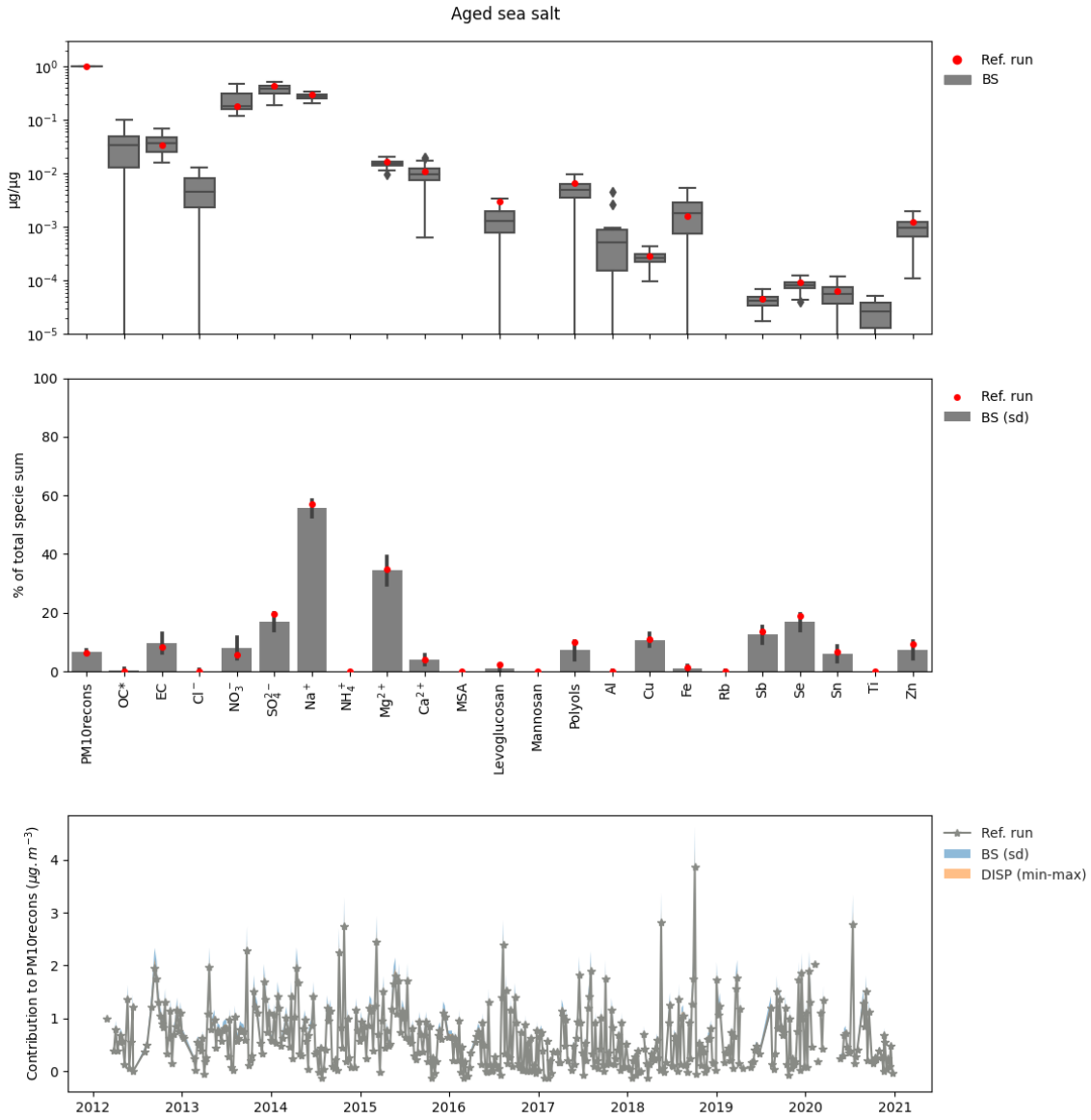

123
124 **Figure S6: Chemical profile and temporal evolution with error estimates of the aged sea salt factor**

125

126

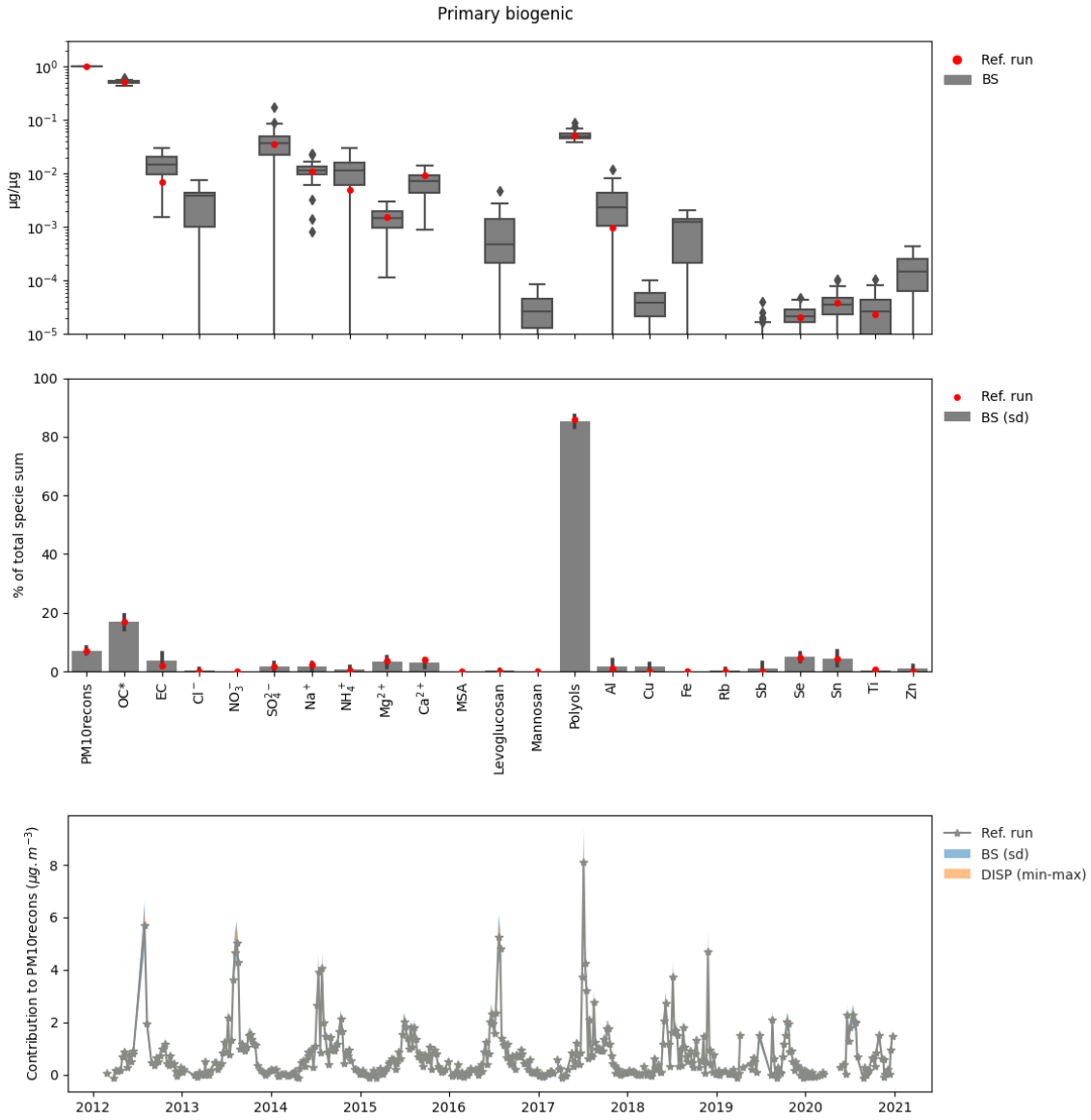

Figure S7: Chemical profile and temporal evolution with error estimates of the primary biogenic factor

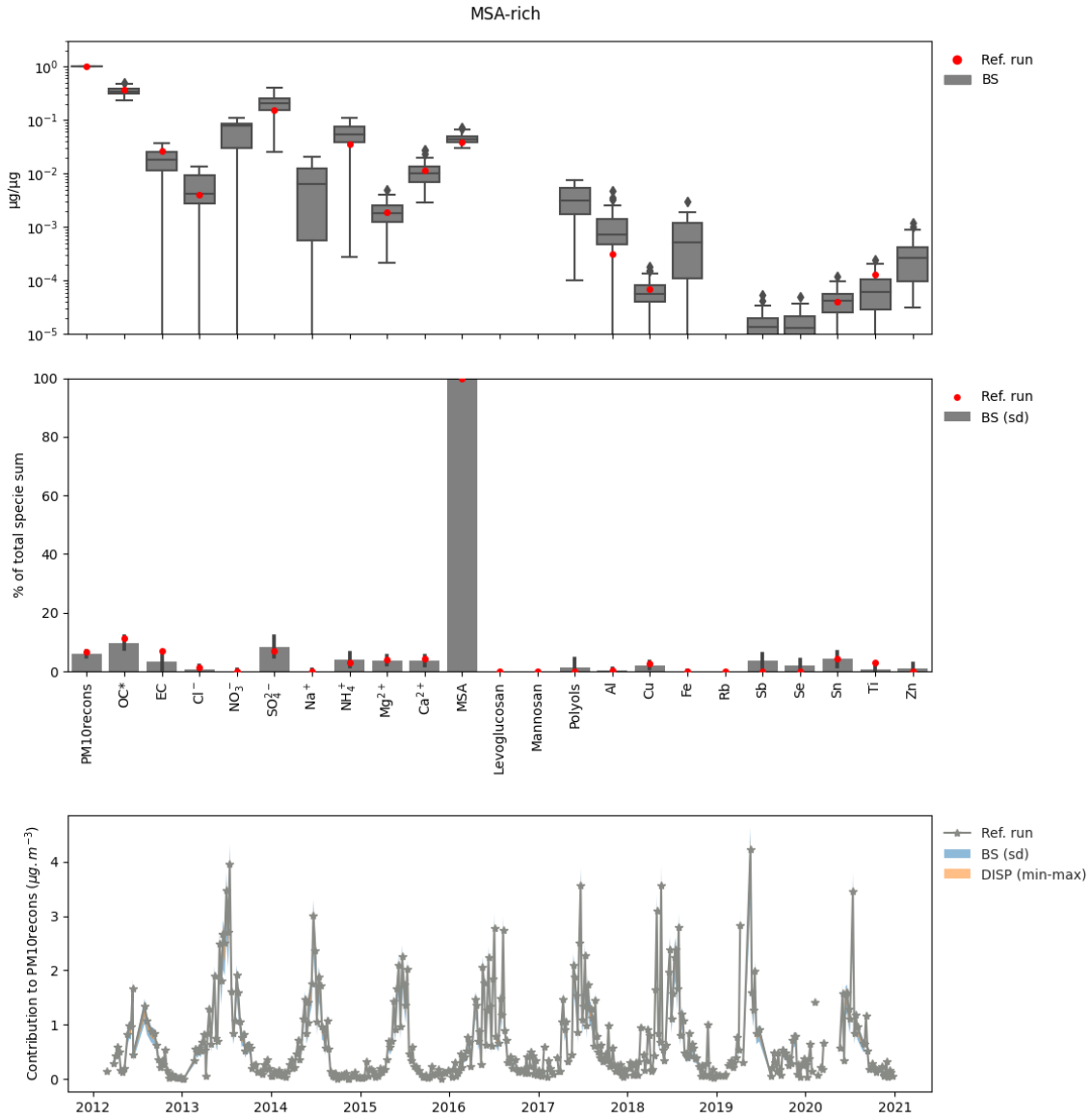

Figure S8: Chemical profile and temporal evolution with error estimates of the MSA-rich factor

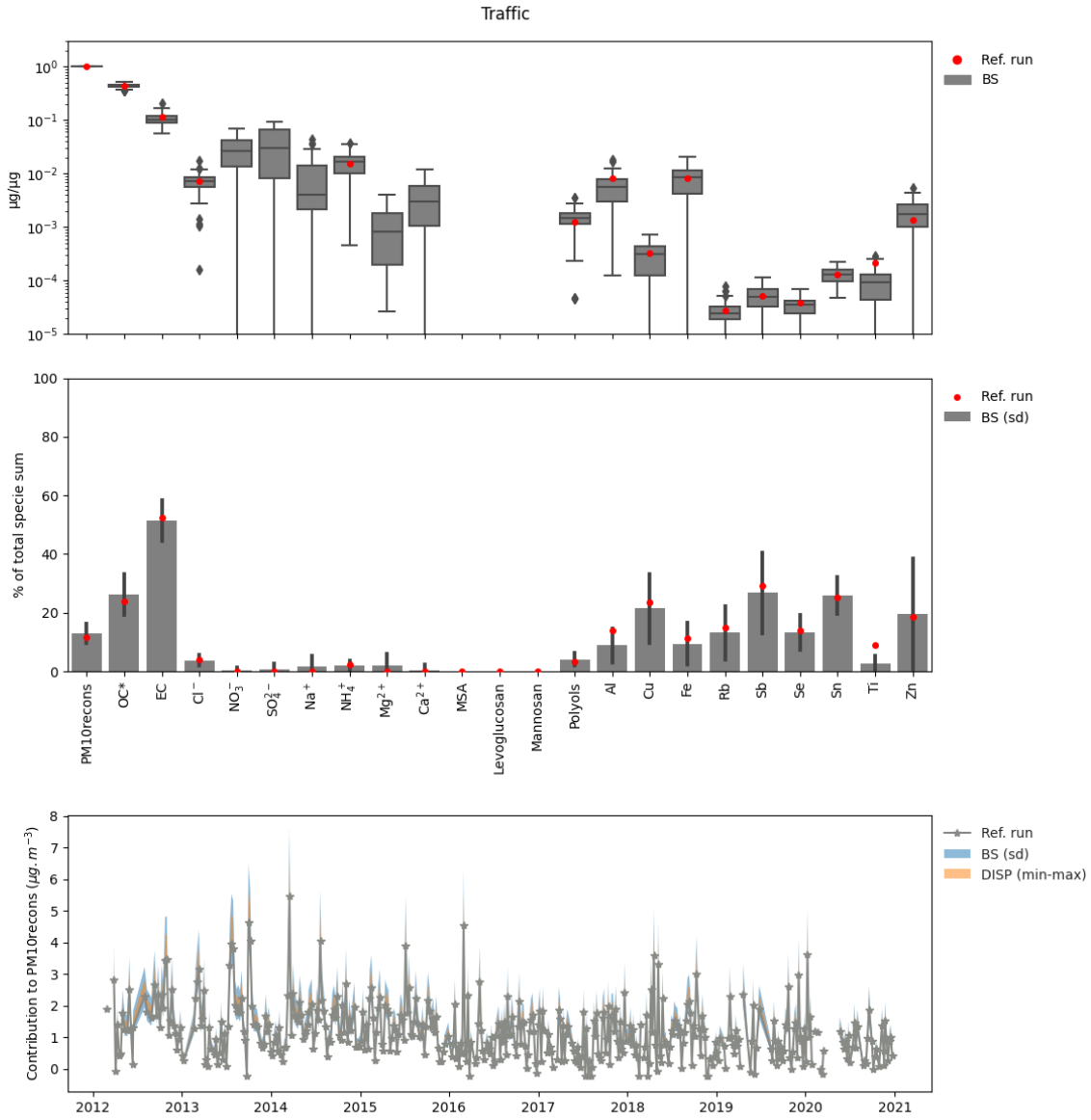

136
137 **Figure S9: Chemical profile and temporal evolution with error estimates of the traffic factor**

138

139

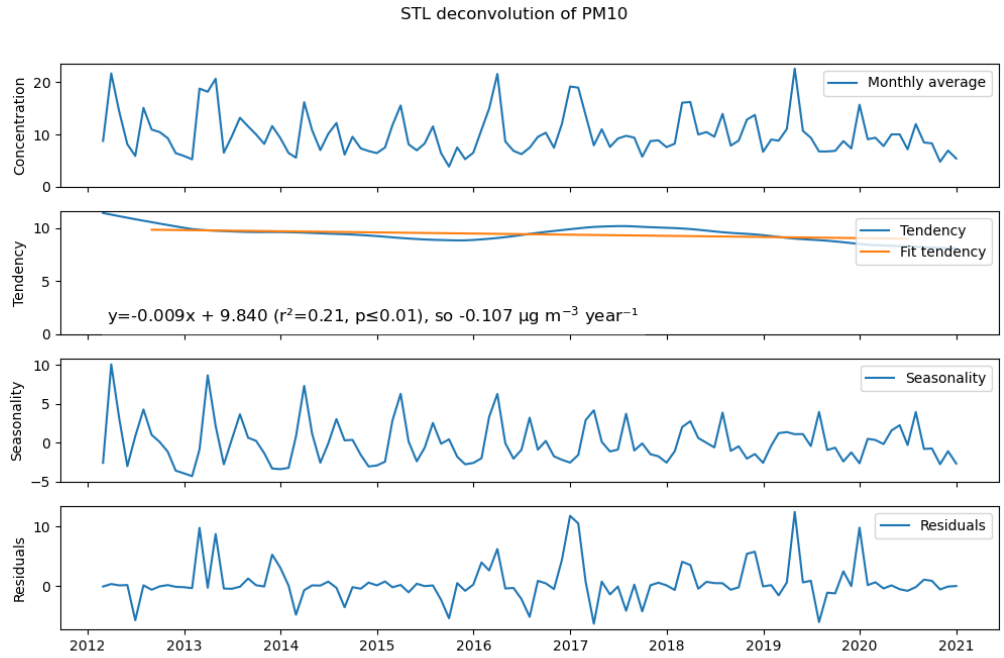

Figure S10: The Season-trend (STL) deconvolution of contributions of PM_{10} in µg m^{-3} from year 2012 to 2020.

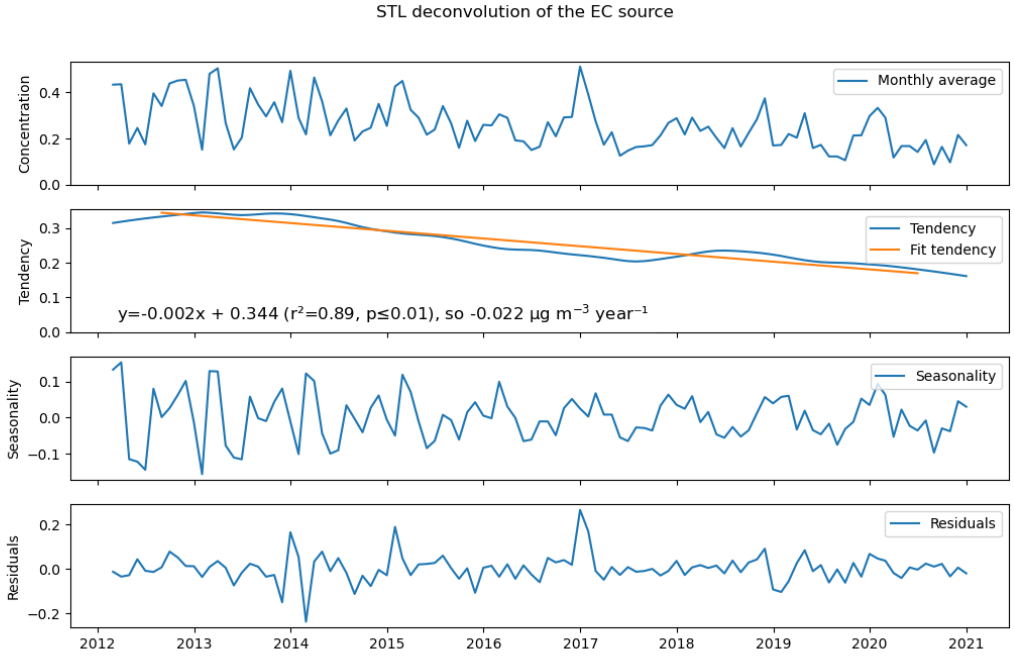

Figure S11: The Season-trend (STL) deconvolution of contributions of EC in µg m^{-3} to PM_{10} from year 2012 to 2020.

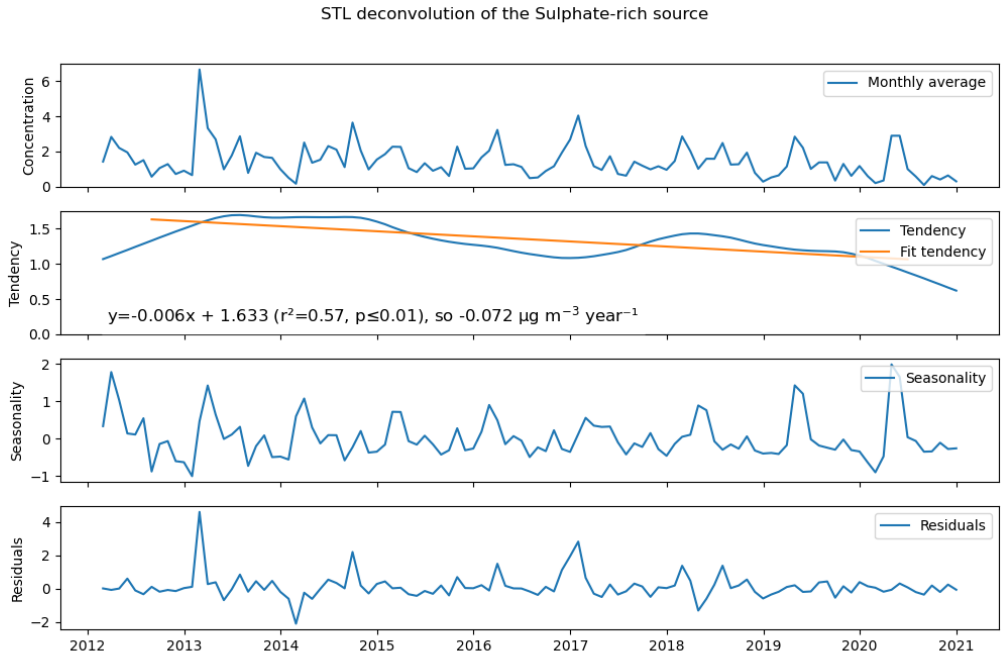

Figure S12: The Season-trend (STL) deconvolution of contributions of EC in µg m^{-3} to PM_{10} from year 2012 to 2020.

Table S4: Comparison of the PMF-resolved source contributions (in terms of µg m^{-3} and percentage) to PM_{10} between daily and weekly samples

Source	24-hr samples (*n*=253)		7-day samples (*n*=181)	
	Contribution (µg m^{-3})	Percentage contribution (%)	Contribution (µg m^{-3})	Percentage contribution (%)
Sulphate-rich	1.5	15.1	1.9	19.7
Primary biogenic	0.6	6.2	1.2	12.4
Aged sea salt	0.9	8.8	0.6	6.2
Nitrate-rich	2.3	22.6	1.7	18.2
Fresh sea salt	0.5	4.6	0.4	4.2
MSA-rich	0.3	3.3	0.5	5.1
Traffic	1.6	15.7	0.9	9.8
Mineral dust	1.2	12.1	1.3	13.8
Biomass burning	1.2	11.7	1.0	10.7

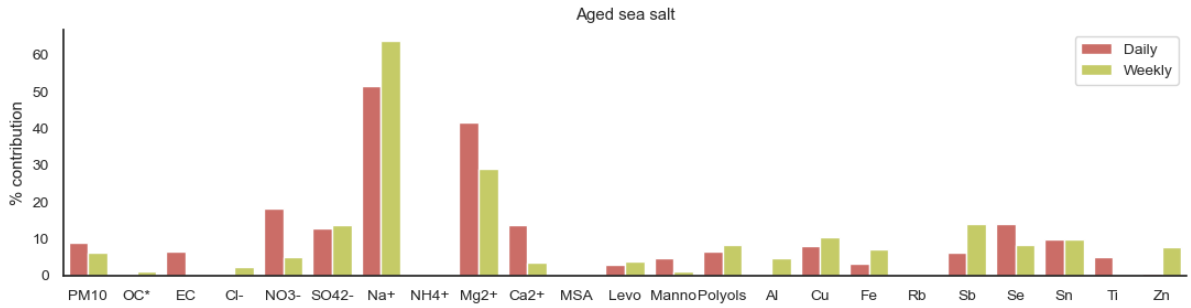

Figure S13: Comparison of PMF-resolved chemical profiles between the weekly (February 28, 2012 to December 28, 2015) and daily (January 12, 2016 to December 22, 2020) samples for the aged sea salt factor. The bars represent the percentage (%) contribution of each specie to total reconstructed PM_{10}.

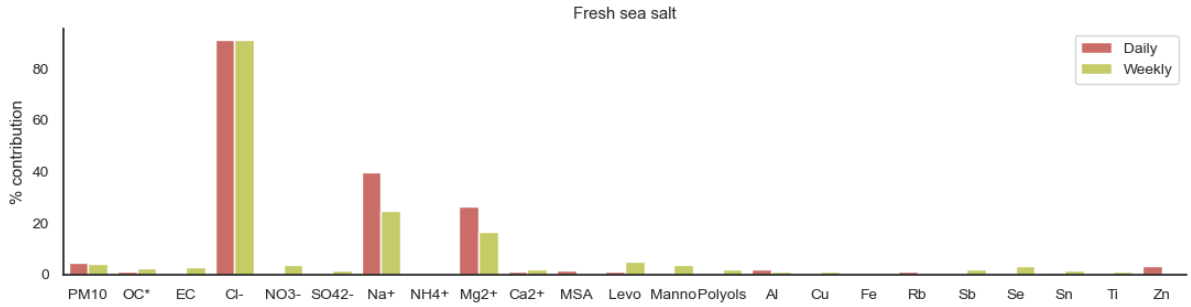

Figure S14: Comparison of PMF-resolved chemical profiles between the weekly (February 28, 2012 to December 28, 2015) and daily (January 12, 2016 to December 22, 2020) samples for the fresh sea salt factor. The bars represent the percentage (%) contribution of each specie to total reconstructed PM_{10}.

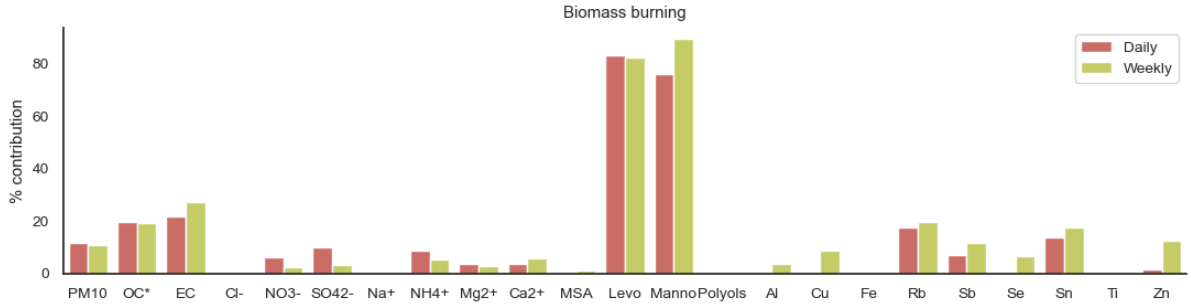

Figure S15: Comparison of PMF-resolved chemical profiles between the weekly (February 28, 2012 to December 28, 2015) and daily (January 12, 2016 to December 22, 2020) samples for the biomass burning factor. The bars represent the percentage (%) contribution of each specie to total reconstructed PM_{10}.

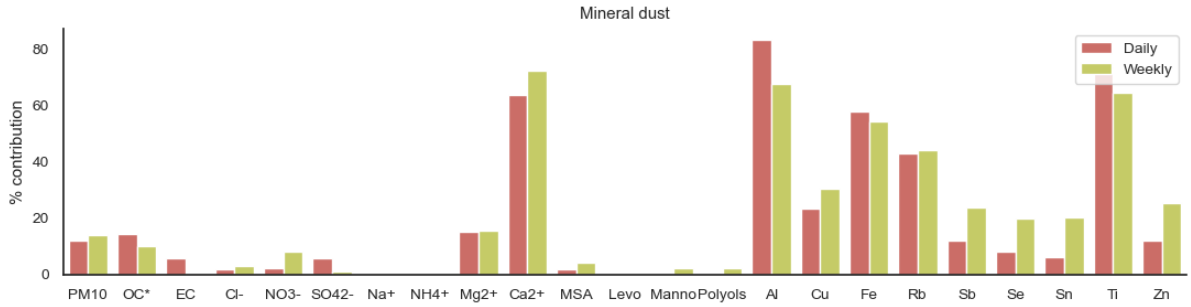

Figure S16: Comparison of PMF-resolved chemical profiles between the weekly (February 28, 2012 to December 28, 2015) and daily (January 12, 2016 to December 22, 2020) samples for the mineral dust factor. The bars represent the percentage (%) contribution of each specie to total reconstructed PM_{10}.

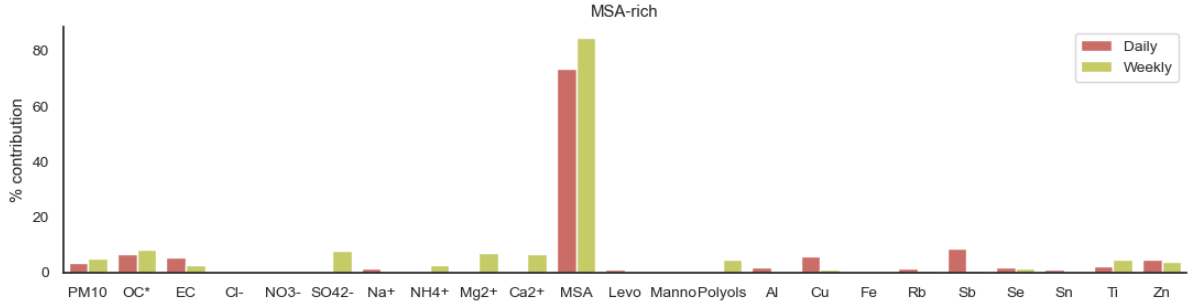

Figure S17: Comparison of PMF-resolved chemical profiles between the weekly (February 28, 2012 to December 28, 2015) and daily (January 12, 2016 to December 22, 2020) samples for the MSA-rich factor. The bars represent the percentage (%) contribution of each specie to total reconstructed PM_{10}.

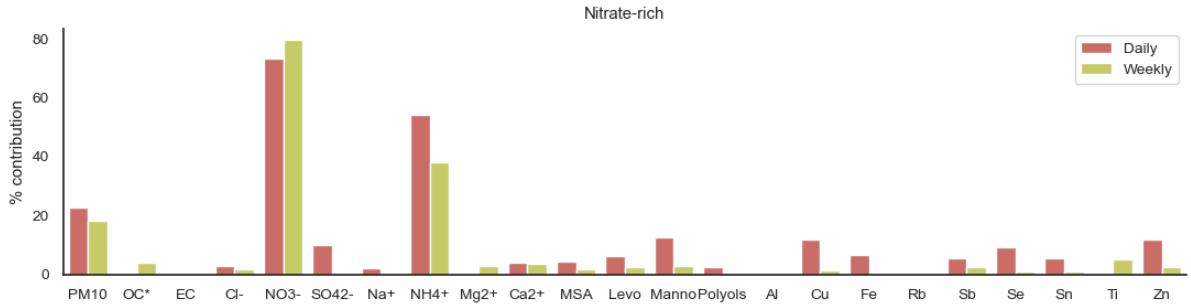

Figure S18: Comparison of PMF-resolved chemical profiles between the weekly (February 28, 2012 to December 28, 2015) and daily (January 12, 2016 to December 22, 2020) samples for the nitrate-rich factor. The bars represent the percentage (%) contribution of each specie to total reconstructed PM_{10}.

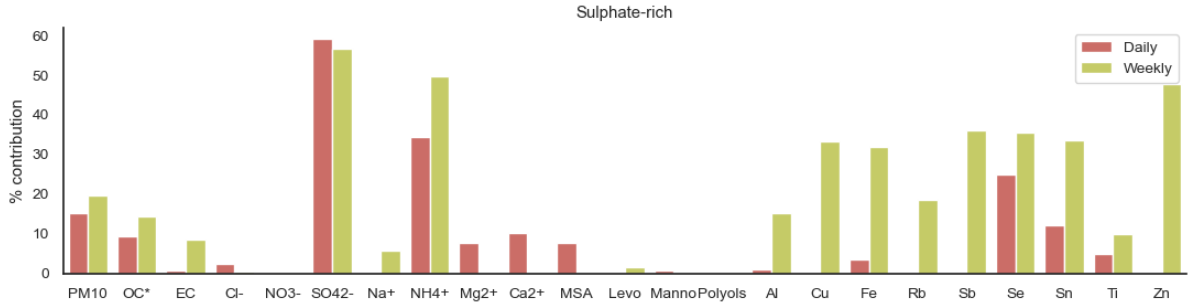

Figure S19: Comparison of PMF-resolved chemical profiles between the weekly (February 28, 2012 to December 28, 2015) and daily (January 12, 2016 to December 22, 2020) samples for the sulphate-rich factor. The bars represent the percentage (%) contribution of each specie to total reconstructed PM_{10}.

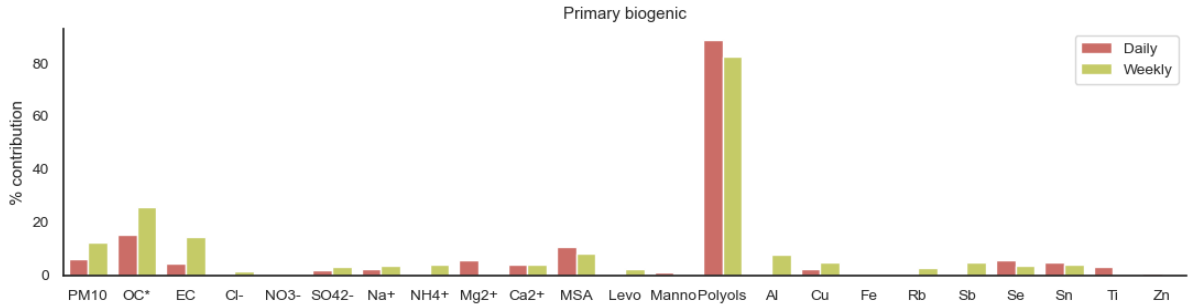

Figure S20: Comparison of PMF-resolved chemical profiles between the weekly (February 28, 2012 to December 28, 2015) and daily (January 12, 2016 to December 22, 2020) samples for the primary biogenic factor. The bars represent the percentage (%) contribution of each specie to total reconstructed PM_{10}.

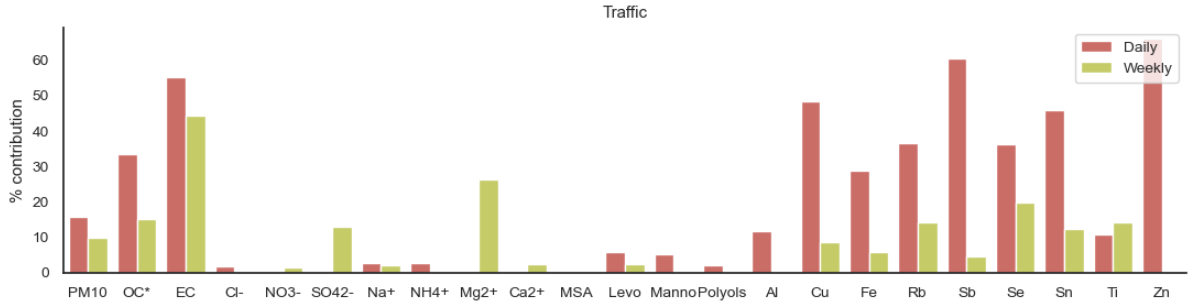

Figure S21: Comparison of PMF-resolved chemical profiles between the weekly (February 28, 2012 to December 28, 2015) and daily (January 12, 2016 to December 22, 2020) samples for the traffic factor. The bars represent the percentage (%) contribution of each specie to total reconstructed PM_{10}.